



Thin Film Ceramic Strain Sensor Development for High Temperature Environments

*John D. Wrbanek and Gustave C. Fralick
Glenn Research Center, Cleveland, Ohio*

*José M. Gonzalez
Gilcrest Electric & Supply Company, Cleveland, Ohio*

*Kimala L. Laster
Sierra Lobo, Inc., Cleveland, Ohio*

NASA STI Program . . . in Profile

Since its founding, NASA has been dedicated to the advancement of aeronautics and space science. The NASA Scientific and Technical Information (STI) program plays a key part in helping NASA maintain this important role.

The NASA STI Program operates under the auspices of the Agency Chief Information Officer. It collects, organizes, provides for archiving, and disseminates NASA's STI. The NASA STI program provides access to the NASA Aeronautics and Space Database and its public interface, the NASA Technical Reports Server, thus providing one of the largest collections of aeronautical and space science STI in the world. Results are published in both non-NASA channels and by NASA in the NASA STI Report Series, which includes the following report types:

- **TECHNICAL PUBLICATION.** Reports of completed research or a major significant phase of research that present the results of NASA programs and include extensive data or theoretical analysis. Includes compilations of significant scientific and technical data and information deemed to be of continuing reference value. NASA counterpart of peer-reviewed formal professional papers but has less stringent limitations on manuscript length and extent of graphic presentations.
- **TECHNICAL MEMORANDUM.** Scientific and technical findings that are preliminary or of specialized interest, e.g., quick release reports, working papers, and bibliographies that contain minimal annotation. Does not contain extensive analysis.
- **CONTRACTOR REPORT.** Scientific and technical findings by NASA-sponsored contractors and grantees.
- **CONFERENCE PUBLICATION.** Collected

papers from scientific and technical conferences, symposia, seminars, or other meetings sponsored or cosponsored by NASA.

- **SPECIAL PUBLICATION.** Scientific, technical, or historical information from NASA programs, projects, and missions, often concerned with subjects having substantial public interest.
- **TECHNICAL TRANSLATION.** English-language translations of foreign scientific and technical material pertinent to NASA's mission.

Specialized services also include creating custom thesauri, building customized databases, organizing and publishing research results.

For more information about the NASA STI program, see the following:

- Access the NASA STI program home page at <http://www.sti.nasa.gov>
- E-mail your question via the Internet to help@sti.nasa.gov
- Fax your question to the NASA STI Help Desk at 301-621-0134
- Telephone the NASA STI Help Desk at 301-621-0390
- Write to:
NASA Center for AeroSpace Information (CASI)
7115 Standard Drive
Hanover, MD 21076-1320



Thin Film Ceramic Strain Sensor Development for High Temperature Environments

*John D. Wrbanek and Gustave C. Fralick
Glenn Research Center, Cleveland, Ohio*

*José M. Gonzalez
Gilcrest Electric & Supply Company, Cleveland, Ohio*

*Kimala L. Laster
Sierra Lobo, Inc., Cleveland, Ohio*

Prepared for the
Aging Aircraft 2008
sponsored by the NASA, FAA, DoD, and ICAA
Phoenix, Arizona, April 21–24, 2008

National Aeronautics and
Space Administration

Glenn Research Center
Cleveland, Ohio 44135

Acknowledgments

We gratefully acknowledge the support of the staff of the NASA GRC Test Facilities Operation, Maintenance, and Engineering (TFOME) organization in maintaining the fabrication and test equipment capabilities of the NASA GRC Microsystems Fabrication Clean Room Facility. We also thank Craig Neslen of the AFRL Nondestructive Evaluation (NDE) Branch and Dr. Gary Hunter of NASA GRC Sensors and Electronics Branch for support and discussions related to this work. Further appreciation is extended to Dr. Otto Gregory of University of Rhode Island Department of Chemical Engineering for his studies in thin film ITO sensors supported by a NASA Research Announcement (NRA) grant.

The work presented here was performed at the NASA Glenn Research Center, sponsored by the Aircraft Aging & Durability (AAD) Project of the Aviation Safety Program as part of the NASA's Aeronautics Research Missions Directorate.

Level of Review: This material has been technically reviewed by technical management.

Available from

NASA Center for Aerospace Information
7115 Standard Drive
Hanover, MD 21076-1320

National Technical Information Service
5285 Port Royal Road
Springfield, VA 22161

Available electronically at <http://gltrs.grc.nasa.gov>

Thin Film Ceramic Strain Sensor Development for High Temperature Environments

John D. Wrbanek and Gustave C. Fralick
National Aeronautics and Space Administration
Glenn Research Center
Cleveland, Ohio 44135

José M. Gonzalez
Gilcrest Electric & Supply Company
Cleveland, Ohio 44135

Kimala L. Laster
Sierra Lobo, Inc.
Cleveland, Ohio 44135

Abstract

The need for sensors to operate in harsh environments is illustrated by the need for measurements in the turbine engine hot section. The degradation and damage that develops over time in hot section components can lead to catastrophic failure. At present, the degradation processes that occur in the harsh hot section environment are poorly characterized, which hinders development of more durable components, and since it is so difficult to model turbine blade temperatures, strains, etc, actual measurements are needed. The need to consider ceramic sensing elements is brought about by the temperature limits of metal thin film sensors in harsh environments. The effort at the NASA Glenn Research Center (GRC) to develop high temperature thin film ceramic static strain gauges for application in turbine engines is described, first in the fan and compressor modules, and then in the hot section. The near-term goal of this research effort was to identify candidate thin film ceramic sensor materials and provide a list of possible thin film ceramic sensor materials and corresponding properties to test for viability. A thorough literature search was conducted for ceramics that have the potential for application as high temperature thin film strain gauges chemically and physically compatible with the NASA GRCs microfabrication procedures and substrate materials. Test results are given for tantalum, titanium and zirconium-based nitride and oxynitride ceramic films.

Nomenclature

| | |
|-----------------------------|--|
| CTE | coefficient of thermal expansion (ppm/°C) |
| TCR | temperature coefficient of resistance (ppm/°C) |
| UHTC | ultra-high temperature ceramic |
| d | film thickness (Å or μm) |
| ϵ | strain; length change per unit length ($\mu\epsilon$) |
| ϵ_a | apparent strain due to temperature rather than applied strain ($\mu\epsilon$) |
| $\delta\epsilon_a/\delta T$ | apparent strain sensitivity to temperature changes ($\mu\epsilon/^\circ\text{C}$) |
| $\delta l/l$ | length change per unit length; strain (ϵ) |
| γ | gauge factor of strain gauge; i.e., the ratio of fractional resistance change to strain |
| $\mu\epsilon$ | unit of microstrain; typically defined as 10^{-6} in. change per inch length ($\mu\text{in./in.}$) |
| ρ | electrical resistivity ($\Omega\text{-cm}$) |
| σ | electrical conductivity ($\Omega\text{-cm}$) ⁻¹ |

1.0 Introduction

1.1 Challenge of Sensors for Propulsion Systems

To advance knowledge in fundamental aeronautics and develop technologies for safer, lighter, quieter, and more fuel efficient aircraft, instrumentation technologies are being developed by the National Aeronautics and Space Administration (NASA) in support of its mission to pioneer the future in space exploration, scientific discovery, and aeronautics research. These technologies also enable the capabilities for long duration, more distant human and robotic missions for the Vision for Space Exploration.

The Sensors and Electronics Branch of the NASA Glenn Research Center (GRC) has an in-house effort to develop thin film sensors for surface measurement in propulsion system research. The sensors include those for strain, temperature, heat flux and surface flow, which will enable critical vehicle health monitoring and characterization of components of future space and air vehicles.

The need for sensors to operate in harsh environments is illustrated by the need for measurements in the turbine engine hot section. The degradation and damage that develops over time in hot section components can lead to catastrophic failure. In fact, turbine engine related class A mishaps are second only to Controlled Flight Into Terrain (CFIT) in their toll on the U.S. Air Force in terms of destroyed and damaged aircraft, and the turbine section of the engine has been consistently responsible for over \$40M in losses a year, more than any other engine component. At present, the degradation processes that occur in the harsh hot section environment are poorly characterized, which hinders development of more durable components, and since it is so difficult to model turbine blade temperatures, strains, etc, actual measurements are needed (ref. 1).

The use of sensors made of thin films has several advantages over wire or foil sensors. Thin film sensors do not require special machining of the components on which they are mounted, and, with thicknesses less than 10 μm , they are considerably thinner than wire or foils. Spray-on sensors with total thicknesses greater than 10 μm are believed to cause increased turbulence and heating of turbine components, thus causing erroneous measurements. Thin film sensors are much less disturbing to the operating environment, therefore having a minimal impact on the physical characteristics of the supporting components.

The need to consider ceramic sensing elements is brought about by the temperature limits of metal thin film sensors in propulsion system applications. Longer-term stability of thin film sensors made of noble metals has been demonstrated at 1100 °C for 25 hr (ref. 2). The capability for thin film sensors to operate in 1500 °C environments for 25 hr or more is considered critical for ceramic turbine engine development (refs. 3 and 4). For future space transportation vehicles, temperatures of propulsion system components over 1650 °C are expected (ref. 5).

1.2 Limits of Metal Film Sensors

A limitation of metal thin films used as sensors to measure strain is that their resistance changes as the temperature changes. This apparent strain (ϵ_a) can be falsely interpreted as actual strain on the component being monitored. For static strain applications for use on gas turbine engines, the current required accuracy is $\pm 200 \mu\text{in./in.} (\mu\epsilon)$ (ref. 6). The thin film palladium-chromium (PdCr) alloy strain gauge, developed at the NASA GRC for high temperature strain measurement applications, is stable to 1100 °C, but has a TCR of 135 ppm/°C and an apparent strain sensitivity ($\delta\epsilon_a/\delta T$) of +85 $\mu\epsilon/^\circ\text{C}$, requiring temperature compensation for high temperature static strain measurements (refs. 2 and 6). Currently, this compensation is in the form of setting a “ballast” potentiometer in a bridge to perform first order elimination of the apparent strain at a particular temperature, but deviations from this matched temperature result in measured apparent strain (ref. 7).

A thin film multifunctional sensor developed at the NASA GRC that can measure directional strain, flow, heat flux, and temperature utilizes this PdCr alloy (ref. 8). It does not incorporate a compensation

bridge in its design but relies on processing the signals from the three elements to compensate for apparent strain.

Nevertheless, a low TCR thin film strain sensor material with thermal stability over a wide range of temperatures would allow high temperature static measurements with the multifunctional sensor as well as a more passive method of eliminating apparent strain without the need for a compensation bridge.

The NASA GRC has thus begun an in-house effort to develop thin film strain sensors with high thermal stability. Ultimately, the goal is to achieve the $\pm 200 \mu\epsilon$ accuracy of measured applied static strain at high temperatures. Assuming that the total signal containing both the applied and apparent strain can be resolved to 1 part in 1000 (i.e., $\delta R/R = 0.001$), and 6 parts in 1000 for a meaningful measurement of applied strain, the apparent strain needs to be limited to less than 30,000 $\mu\epsilon$ over the temperature range of use. Using the desired 1500 °C range, the apparent strain sensitivity to temperature is then to be less than $\pm 20 \mu\epsilon/^\circ\text{C}$. Increasing the resolution of the signal or decreasing the use range will increase the desired apparent strain sensitivity. As this goal is approached, the drift strain (creep) will also be considered as part of the total strain measurement.

2.0 Ceramic-Based Thin Film Sensor Development

2.1 Background

Since 1991, there have been many investigations into the application of ceramic thin films for use as high temperature thin film strain gauges. A summary of notable high temperature thin film strain gauges is given in table 1. Thin film resistors for regulating electronics based on doped nickel-chromium alloy films with a TCR of $\pm 5 \text{ ppm}/^\circ\text{C}$ and greater are common in the electronics industry, but they are generally restricted to a temperature range between -55 to 125°C (ref. 9), and thus not suitable for our applications.

TABLE 1.—A REVIEW OF HIGH TEMPERATURE THIN FILM STRAIN GAUGE ATTRIBUTES

| Gauge material | TCR, (ppm/°C) | Gauge factor, (γ), ($\delta R/R \cdot \epsilon$) | Apparent strain sensitivity, ($\mu\epsilon/^\circ\text{C}$) | Maximum use temperature, (if reported), (°C) | Fabrication notes | Ref. |
|----------------------|---------------|---|---|--|---|-------|
| Ni-20%Cr | 290 | 2.5 | 116 | 700 | COTS standard | 17,18 |
| Pd-13%Cr | 135 | 2 to 1.4 | 85 | 1100 | THE NASA standard | 2 |
| AlN | -1281 to 109 | 3.72 to 15 | -344 to 29 | >1100 | Al reacted with N | 19 |
| ITO | -469 to 230 | -6.5 to -11.4 | -35 to 72 | >1100 | Oxygen doping | 20 |
| Al:ITO | -1200 | 8 | -150 | 1280 | Aluminum doping | 21 |
| N:TiB ₂ | -50 | 1.4 | -36 | <3225 | Nitrogen doping | 22 |
| Cu:Ta ₂ N | -800 to 200 | 2.3 to 5.1 | -348 to 87 | (not reported) | Ta reacted w/ N; Cu doping | 23 |
| Ta ₂ N | -80 | 3.5 | -23 | (not reported) | Ta reacted with N | 24 |
| TaON | -290 | 3.5 | -83 | (not reported) | Ta reacted with N; 1% Ox | 25 |
| TiB ₂ | 36 | (not reported) | ----- | <2970 | Ti reacted with B ₂ H ₆ | 26 |
| ZrN | 184 to 275 | (not reported) | ----- | <2980 | Zr reacted with N | 26 |

The gauge factor (γ) of the strain gauge relates the sensitivity of the gauge to strain ($\epsilon = \delta l/l$), as shown in eq. (1).

$$\gamma\epsilon = \gamma \frac{\delta l}{l} = \frac{\delta R}{R} \quad (1)$$

The apparent strain sensitivity to temperature ($\delta\epsilon_a/\delta T$) is the TCR divided by the gauge factor plus the difference in the substrate and the gauge material's CTE, as shown in eq. (2). The difference in the CTEs is expected to be less than 5 ppm/°C based on the materials that we are exploring, and this will be left as an uncertainty in our apparent strain calculation.

$$\frac{\delta\epsilon_a}{\delta T} = \frac{\text{TCR}}{\gamma} + \Delta\text{CTE} \quad (2)$$

Based on the thin film gauges reported in the references shown in table 1, aluminum nitride (AlN), indium-tin oxide (ITO), titanium boride (TiB₂), and doped and undoped tantalum nitride (TaN) and titanium nitride (TiN) are obvious candidates for use for static strain measurements using the apparent strain sensitivity as a guide. Though no gauge factors were reported, zirconium nitride (ZrN) is also attractive since the TCR can be modified through the reactive sputtering process. The maximum use temperature of TaN may be up to 2000 °C, the most attractive for high temperature applications. As a thin film, TaN is known as a stable high temperature resistor with a TCR between 200 and –200 ppm/°C. The TCR depends on the fabrication process, nitride phase produced (e.g., Ta₂N, TaN, Ta₅N₆, etc.), incorporation of oxide on the TaN grains and the degree of amorphous structure (refs. 10 to 13).

To be compatible with our patterning processes, AlN was eliminated from our list of potential candidates as it decomposes in water. Also, the modification of films with oxygen, nitrogen or aluminum doping for electrical properties, such as TCR or resistivity, is common. The report of studies (ref. 14) of resistors using NiCr and TaNiCr interlayers with TaN to achieve TCR between 5 and –5 ppm/°C began our investigation to develop a tantalum nitride film for use with the PdCr strain gauge to achieve the passive elimination of apparent strain sensitivity (ref. 15). The conductive ceramics of titanium and zirconium were identified as candidates for high temperature strain gauge applications and examined in parallel with the TaN runs (ref. 16).

2.2 Tantalum Nitride Film Fabrication

The first step to developing an interlayered or multilayered TaN/PdCr film was to develop a process to reactively sputter the tantalum nitride consistently (ref. 15). The first depositions were on alumina substrates using a 3 in. unbalanced magnetron source and a 99.95 percent pure tantalum target sputtered in an argon/nitrogen atmosphere. The resulting film resistivities of the samples were measured using a four-point probe (ref. 27) with spacing of 2.54 mm. Based on the result of these initial runs, a multifunctional sensor (sample JG40922) with a length to width ratio (l/w) of 290 of tantalum nitride was patterned using the sacrificial-layer lift-off process that is used for microfabricated noble-metal sensors of fine line widths (ref. 28). The completed sensor is shown in figure 1. The TCR was measured to be –93 ppm/°C, and the resistivity 259 $\mu\Omega$ -cm. The strain sensitivity was measured using the algorithm developed for the sensor (ref. 8). A graph showing the fractional change in gauge resistance ($\delta R/R$) versus the applied strain is shown in figure 2. From eq. (1), the gauge factor is found from the slope of the line fitted to the data. The gauge factor was found to be 3.9 ± 0.1 , with the angle resolution determined to be less than $\pm 0.2^\circ$. This translates to an apparent strain sensitivity of $-24 \mu\epsilon/^\circ\text{C}$, similar to what was reported by Ayerdi, et al. (ref. 24) and close to our goal of less than $\pm 20 \mu\epsilon/^\circ\text{C}$.

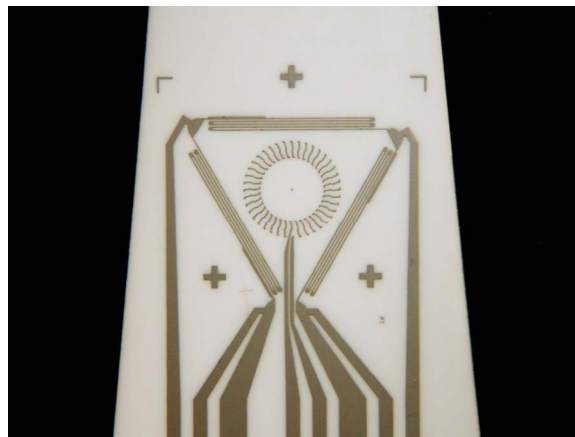


Figure 1.—TaN Multifunctional Sensor.
(Patterned by Photolithography)

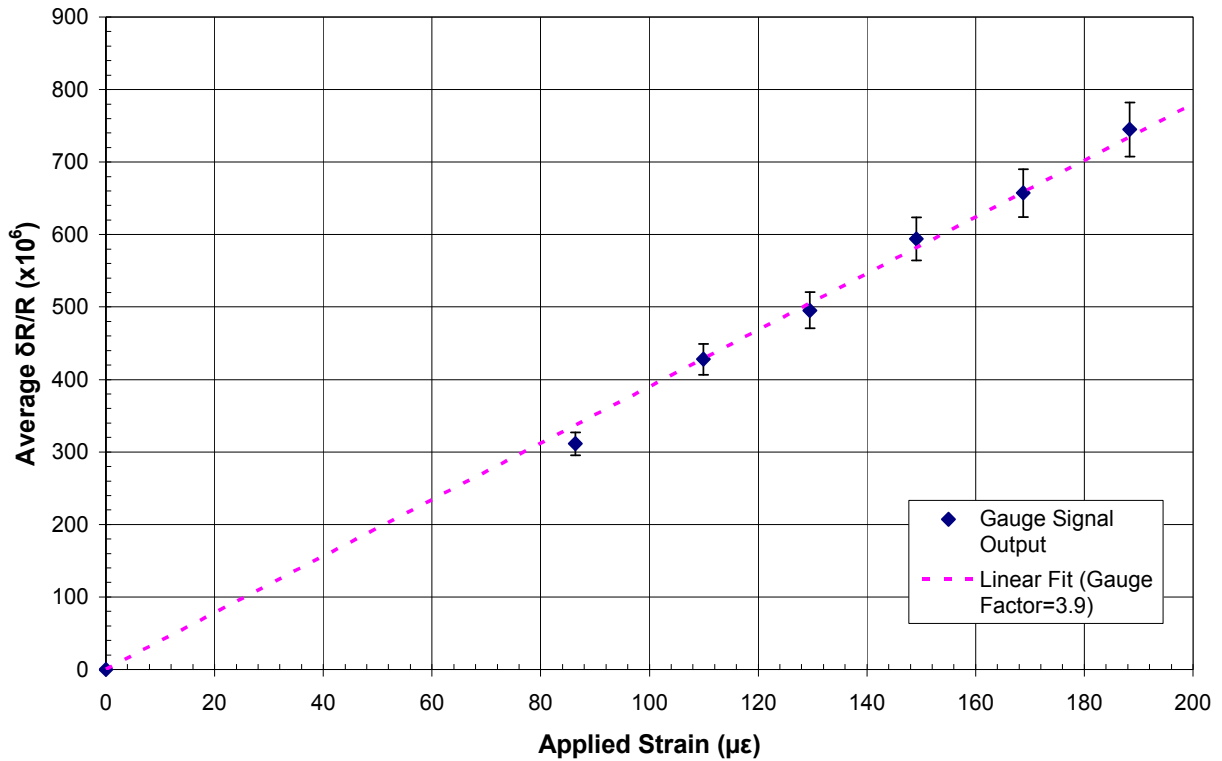


Figure 2.—Strain output of the TaN multifunctional sensor (sample JG40922) at room temperature. Error bars reflect ± 5 percent uncertainty in the measurement.

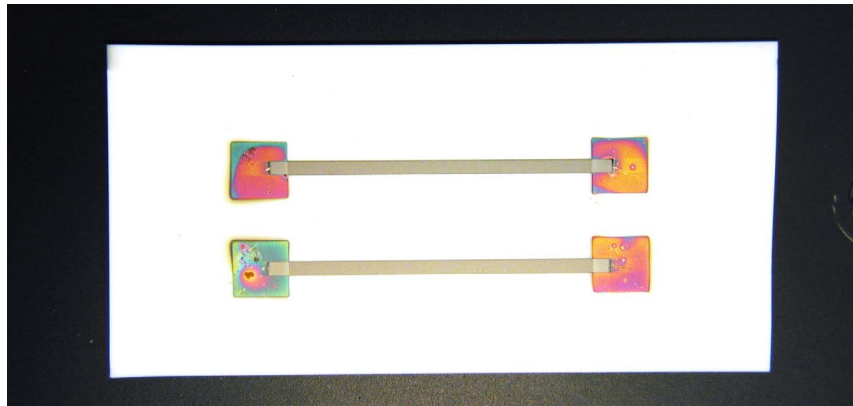


Figure 3.—Ceramic sensor shadow-masked samples.

Target arcing and degradation, however, was becoming an issue, with the thickness of the sensor of run JG40922 about 20 percent less than the initial runs of unpatterned sensors. For the next set of runs, the system pressure and power were lowered to prevent the arcing and degradation of the tantalum target. The films were patterned using a shadow mask with $l/w = 21.88$ (shown in fig. 3), allowing the resistivity to be measured as well as the TCR using a four wire method with a data acquisition system. The resulting

optimized film of run JG50115 had a TCR of $-200 \text{ ppm}/^{\circ}\text{C}$ and a resistivity of $155 \text{ }\mu\Omega\text{-cm}$, a candidate for passive compensation using PdCr. The parameters of the optimized runs for photolithographic and shadow-masked patterns are given in table 2.

TABLE 2.—OPTIMIZED TANTALUM NITRIDE DEPOSITIONS USING PHOTOLITHOGRAPHY AND SHADOWMASK

| Sample | RF power, (W) | Process pressure, (mTorr) | Argon flow, (sccm) | Nitrogen flow, (sccm) | Run time, (sec) | Film thickness, (μm) | Resistivity, ρ , ($\mu\Omega\text{-cm}$) | TCR, ($\text{ppm}/^{\circ}\text{C}$) |
|----------------------------|---------------|---------------------------|--------------------|-----------------------|-----------------|-----------------------------------|---|--|
| JG40922 (Photolithography) | 250 | 8 | 38 | 2 | 7200 | 3.9 | 259 | -93 |
| JG50115 (Shadow-mask) | 125 | 2 | 38 | 2 | 3600 | 1.0 | 155 | -200 |

2.3 Nitride Films with Titanium and Zirconium

Besides tantalum, conductive ceramics of titanium and zirconium were identified as candidates for high temperature strain gauge applications (ref. 16). The examination of the nitrides of titanium was begun in parallel with the TaN runs. The initial runs were to provide a test of the TCR at low temperatures to 200°C on a hot plate, providing the first level of optimizing the resistivity and deposition rate of films patterned by photolithography. The pattern had an $l/w = 250$, and is shown in figure 4.

All samples were fabricated using a 3 in. unbalanced magnetron source at 125W RF, and vacuum annealed at 600°C for 8 hr before hot plate testing. As a baseline comparison for determining an appropriate recipe for the ceramic films, an initial sample of undoped Ti using a 99.99 percent pure target was deposited. The resistivity, TCR as well as the repeatability in resistance was measured in two data collection runs. Several runs were conducted using different partial pressures of nitrogen and oxygen while sputtering. To keep the pressure to manageable levels in the sputtering system, flows were limited to 40 sccm for 2 mTorr, and 20 sccm for 1 mTorr system pressures. The amount of reactive gas to the system was set to 0, 1, or 2 sccm for nitrogen and 0 or 0.5 sccm for oxygen; greater flows of each were found to result in insulating films.

The reactive gas flow was modified for each run to allow optimizing the deposition time and resistivity to give indication of nitride and oxide formation. Matrix fits using process optimization are shown in figures 5 and 6. The resulting film parameters and properties are shown in table 3. Since the results were consistent with the TaN films, these run parameters were then used for zirconium-based reacted films, also shown in table 3.

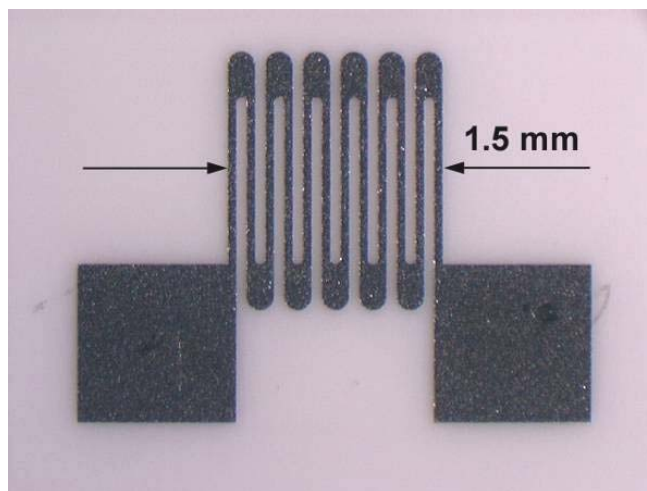


Figure 4.—Ceramic sensor samples patterned by photolithography.

Fit of Film Deposition Rate vs. Reacting Gas Partial Pressures ($\pm 6.5 \text{ \AA/min}$)

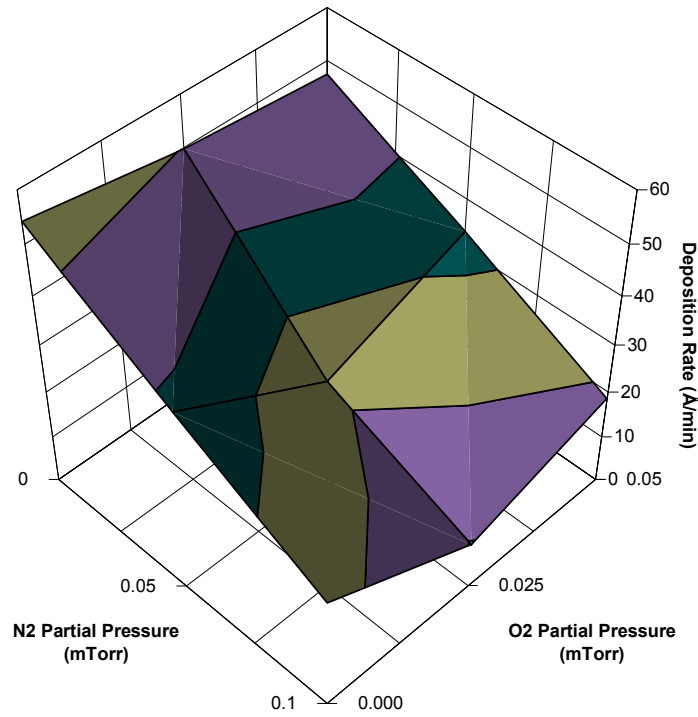


Figure 5.—Deposition rate versus reacting gas pressures to determine gas mixes for optimal deposition rate in reacted films.

Fit of Film Resistivity vs. Reacting Gas Partial Pressures ($\pm 1470 \mu\Omega\text{-cm}$)

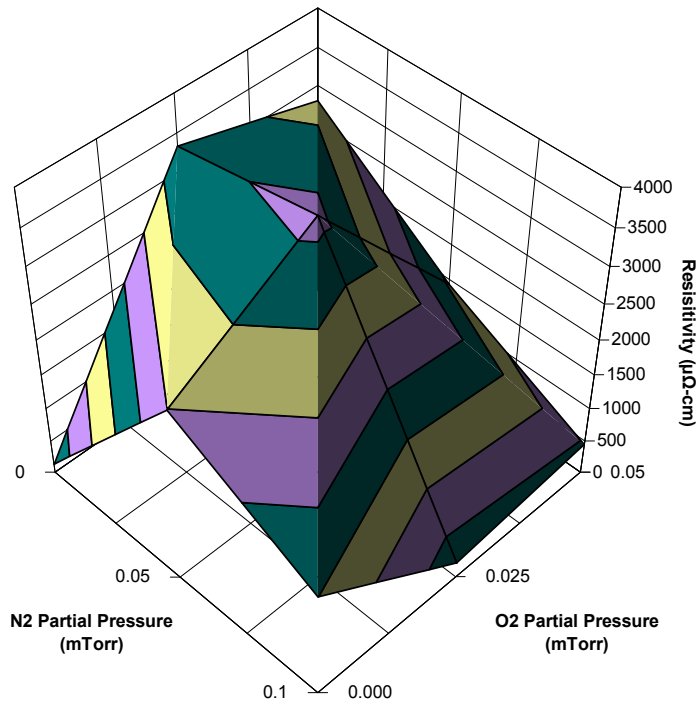


Figure 6.—Resistivity versus reacting gas pressures to determine gas mixes for optimal resistivity. The peak indicates a well-reacted ceramic.

TABLE 3.—PROPERTIES OF METALLIC AND METAL-DERIVED THIN FILMS

| Film | Ar/N/O gas flow mix | Deposition time, (min) | Thickness, ($\pm 0.1 \mu\text{m}$), (μm) | Resistivity, ($\pm 10\%$), ($\mu\Omega\text{-cm}$) | TCR, ($\pm 10 \text{ ppm}/^\circ\text{C}$) ($\text{ppm}/^\circ\text{C}$) | $\Delta R_o/R_o$ for 200 $^\circ\text{C}$ cycle, (%) |
|----------|---------------------|------------------------|---|--|--|--|
| Ti | 40/0/0 | 369 | 2.0 | 133 | 1,360 | 4.45 |
| TiN | 38/2/0 | 1,200 | 2.8 | 1,490 | 624 | 114 |
| TiON | 18/1/0.5 | 360 | 0.6 | 62 | 1,400 | 0.83 |
| Zr | 40/0/0 | 198 | 2.0 | 140 | 1,090 | 2.73 |
| ZrN | 38/2/0 | 750 | 2.4 | 1,090 | 146 | 4.26 |
| ZrON | 18/1/0.5 | 360 | 1.7 | 82 | 695 | -1.3 |
| TiAlCr | 20/0/0 | 360 | 2.1 | 156 | -124 | 2.89 |
| TiAlCrN | 38/2/0 | 595 | 2.0 | 300,000 | -1,342 | 260 |
| TiAlCrON | 18/1/0.5 | 450 | 2.4 | 4,480 | 841 | 23.2 |

To investigate the addition of aluminum to titanium, a 3 in. target of titanium with 51 percent aluminum and 12 percent chromium by weight (99.99 percent purity) ($\text{Ti}_{0.27}\text{Al}_{0.66}\text{Cr}_{0.07}$) was purchased. The target alloy was chosen based on the reported oxidation resistance of the alloy when used as a coating at high temperatures (ref. 29). The alloy was then used as the base of nitride films included as well in table 3.

Nitrogen doping produced films with lower TCR, but the TCR was still above the value that could be compensated in signal conditioning. The nitride films were, however, more unstable in air. The oxynitride films produced a more stable film in air, but they did not have the TCR improvement that was hoped. Further, the TiAlCrON film was more unstable in oxygen than the un-doped original. The un-doped TiAlCr film had a similar negative TCR to the positive value of ZrN, and the stabilities of the films were similar in air. These characterizations of TiAlCr and ZrN films lead directly to examining these two films as a compensating pair for strain gauges.

3.0 Multilayered Film Fabrication

3.1 Multilayer Film Approach

Once the TaN film deposition parameters were finalized, the multilayered TaN/PdCr films were attempted (ref. 15). A cross-section schematic of the multilayered film is shown in figure 7. As an estimate for the relative thicknesses, the assumption is made that because the film thicknesses (d) are greater than the grain size, and thus electron mean free path, the films can be treated as three independent layers in parallel (to first approximation) (ref. 30).

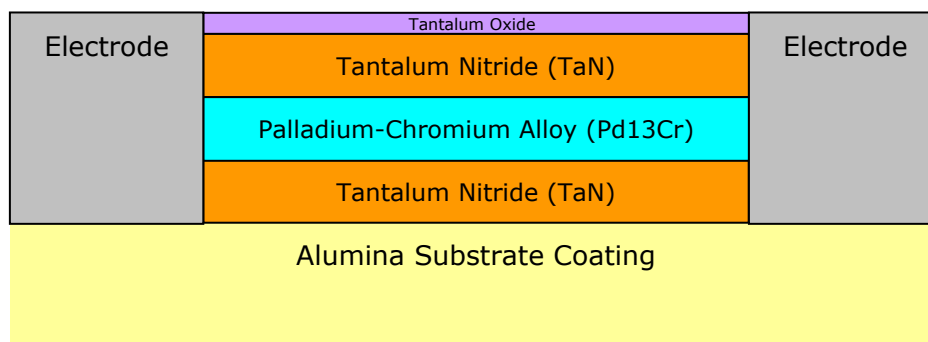


Figure 7.—A cross-section schematic of the multilayer thin film sensor.

The conductivity (σ) is the inverse of the resistivity (ρ), and because the first and last layers are the same material (TaN) and the second is PdCr, the conductivities add as in eq. (3).

$$\sigma_{\text{Total}} = \sigma_{\text{TaN}} \frac{d_{\text{TaN}}}{d_{\text{Total}}} + \sigma_{\text{PdCr}} \frac{d_{\text{PdCr}}}{d_{\text{Total}}} \quad (3)$$

Similarly, the TCR (α) for multiple layers is derived as in eq. (4).

$$\alpha_{\text{Total}} = \frac{d_{\text{TaN}} \sigma_{\text{TaN}} \alpha_{\text{TaN}} + d_{\text{PdCr}} \sigma_{\text{PdCr}} \alpha_{\text{PdCr}}}{d_{\text{TaN}} \sigma_{\text{TaN}} + d_{\text{PdCr}} \sigma_{\text{PdCr}}} = \frac{d_{\text{TaN}} \sigma_{\text{TaN}} \alpha_{\text{TaN}} + d_{\text{PdCr}} \sigma_{\text{PdCr}} \alpha_{\text{PdCr}}}{d_{\text{Total}} \sigma_{\text{Total}}} \quad (4)$$

To cancel out the TCR ($\alpha_{\text{Total}}=0$), the numerator is set to zero, as shown in eq. (5).

$$d_{\text{TaN}} \sigma_{\text{TaN}} \alpha_{\text{TaN}} = -d_{\text{PdCr}} \sigma_{\text{PdCr}} \alpha_{\text{PdCr}} \quad (5)$$

The ratio of PdCr film thickness to TaN film thickness then can be derived in eq. (6).

$$\frac{d_{\text{PdCr}}}{d_{\text{TaN}}} = -\frac{\sigma_{\text{TaN}}}{\sigma_{\text{PdCr}}} \frac{\alpha_{\text{TaN}}}{\alpha_{\text{PdCr}}} = -\frac{\rho_{\text{PdCr}}}{\rho_{\text{TaN}}} \frac{\alpha_{\text{TaN}}}{\alpha_{\text{PdCr}}} \quad (6)$$

So, to a first approximation, the TCR of the multilayer can be minimized with the knowledge of the resistivity and TCR of the component films. Using the values of TaN from JG50115 in table 2, and the resistivity and TCR of PdCr as 110 $\mu\Omega\text{-cm}$ and 170 ppm/ $^{\circ}\text{C}$ respectively, the ratio of PdCr to TaN thickness to cancel the multilayer film TCR is found to be 0.835.

As TaN films seem to vary more than annealed metallic films from bulk values in literature (refs. 10 to 13, and 31), the determination of the resistivity and TCR of the TaN film layers of the multilayer films shed light on the variation of the parameters for TaN for these runs. From eqs. (3) and (4), the TCR and resistivity of the TaN portion of the films formed in the multilayer can be determined.

Since the thicknesses of the films individually are measured, as is the total conductivity and TCR (as shown in table 3), the TaN conductivity can be estimated from eq. (3):

$$\sigma_{\text{TaN}} = \frac{\sigma_{\text{Total}} d_{\text{Total}} - \sigma_{\text{PdCr}} d_{\text{PdCr}}}{d_{\text{TaN}}} \quad (7)$$

Likewise, the TCR can be estimated from eq. (4):

$$\alpha_{\text{TaN}} = \frac{d_{\text{Total}} \sigma_{\text{Total}} \alpha_{\text{Total}} - d_{\text{PdCr}} \sigma_{\text{PdCr}} \alpha_{\text{PdCr}}}{\sigma_{\text{TaN}} d_{\text{TaN}}} \quad (8)$$

3.2 Multilayered Film Samples

Multiple sets of TaN/PdCr multilayer films were fabricated with different PdCr to TaN thicknesses, with each set having two samples using identical machine parameters. The films were patterned using a shadow mask with $l/w = 21.88$ as shown in figure 3, allowing the resistivity to be measured as well as the TCR using a four wire method with a data acquisition system. From this data, the resistivity and TCR from the TaN film in the multilayer was determined to be $199 \pm 24 \mu\Omega\text{-cm}$ and $-130 \pm 30 \text{ ppm}/^{\circ}\text{C}$, shown as the “best fit” curves in figures 8 and 9. The TCR and resistivity for the TaN films for one sample in the figures is observed to be more similar to Ta+TaN mixed films than to pure TaN films, and was not included in the “best fit” curve.

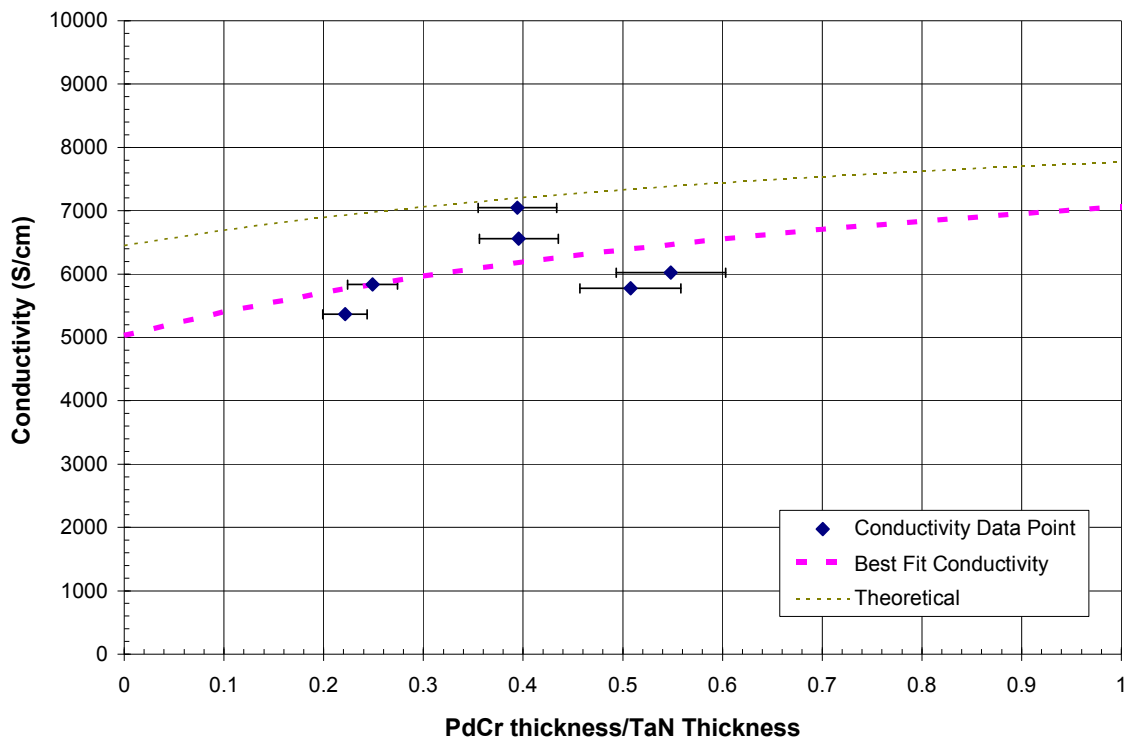


Figure 8.—Conductivity of TaN/PdCr multilayer at room temperature versus PdCr/TaN thickness ratio.

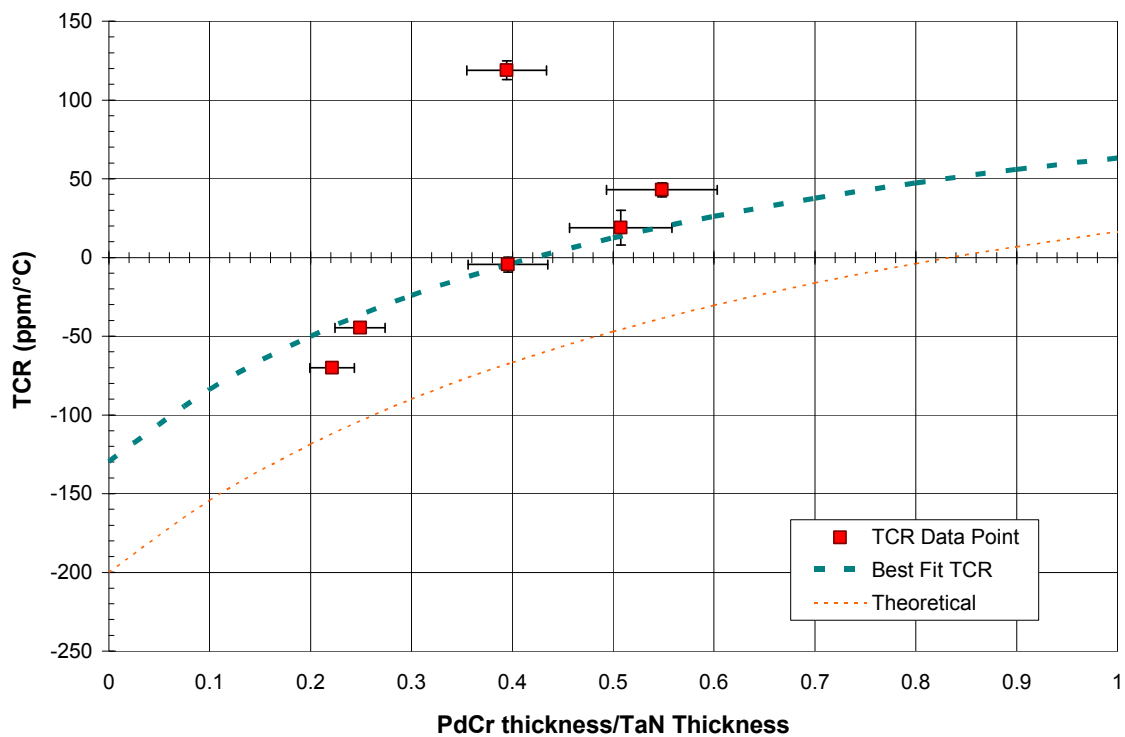


Figure 9.—TCR of TaN/PdCr multilayer versus PdCr/TaN thickness ratio.

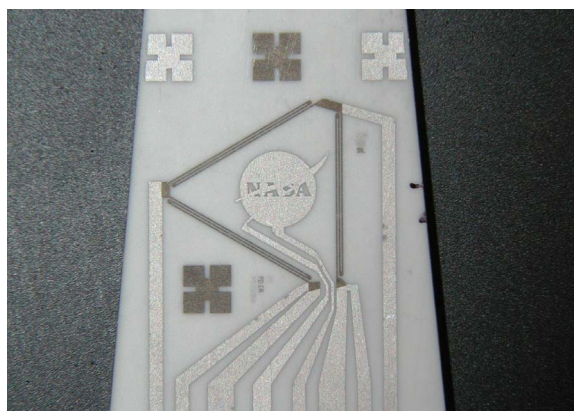


Figure 10.—TaN/PdCr multilayer multifunctional sensor rosette.

3.3 Multilayered TaN/PdCr Multifunctional Sensor Application

To test the TaN/PdCr multilayer as multifunctional sensors, several multifunctional sensors were fabricated using the pattern shown in figure 10 with $l/w = 447$. The properties of the optimized sensor (JG60522) are summarized in table 5, which also contains the pure TaN multifunctional sensor (JG40922) as a reference. The optimized sample has a PdCr to TaN ratio of 0.86, which reflects the suspected incorporation of oxygen into the multilayer film through our sacrificial copper/nitric acid etch lithographic process that is used to pattern the sensors. The sensor was annealed in vacuum at 600 °C for 8 hr before testing. The resistivity and gauge factor were low, reflecting the PdCr layer. The TCR varied between 0 and 30 ppm/°C over a temperature range of 20 to 120°C. The temperature was measured through the use of an external thermocouple in contact with the sample in the oven since the leadwires broke to the on-sample pattern thermocouple. The leadwires were repaired, and another round of tests was conducted to 600 °C, which resulted in a higher resistivity and a TCR of 328 ppm/°C. The gauge factor also increased to 2.1, suggesting that the TaN was not stable under high temperature conditions over 500 °C in air.

TABLE 5.—TaN/PdCr MULTILAYER MULTIFUNCTIONAL SENSOR SAMPLE PROPERTY SUMMARY

| Sample | TaN thickness, (± 250 Å), (Å) | PdCr thickness, (± 250 Å), (Å) | TaN+TaO thickness, (± 250 Å), (Å) | Sample resistivity, ($\pm 5\%$), ($\mu\Omega$ -cm) | Sample TCR, (± 5 ppm/°C), (ppm/°C) | Gauge factor, ($\pm 5\%$), ($\delta R/R/\epsilon$) | Apparent strain sensitivity, ($\pm 10\%$), ($\mu\epsilon/^\circ\text{C}$) |
|---------------------|------------------------------------|-------------------------------------|--|---|---|--|---|
| JG40922 | 39,000 | ----- | ----- | 259 | -93 | 3.9 | -24 |
| JG60522 (to 120 °C) | 2900 | 4600 | 3450 | 146 | 15 \pm 15 | 1.23 | 12 \pm 12 |
| JG60522 (to 600 °C) | 2900 | 4600 | 3450 | 444 | 328 | 2.1 | 156 |

3.4 Multilayered ZrN/TiAlCr Multifunctional Sensor Application

Multilayered sensors using ZrN and TiAlCr films were fabricated as well using the pattern shown in figure 10 with $l/w = 447$. The film thicknesses were established based on the results in table 3 using ZrON as an overcoat for KL70413, and an oxidized PtAl overcoat for KL71024. The results of these multilayered sensors are shown in table 6. The substrate of the first sample broke when strained, and the second sample showed a reasonable gauge factor for a multilayered film. However, both films were not stable even under low temperature heating, having excessive TCRs for use as strain gauges.

TABLE 6.—ZrN/TiAl MULTILAYER SAMPLE PROPERTIES

| Sample | Layer 1, (± 250 Å), (Å) | Layer 2, (± 250 Å), (Å) | Layer 3, (± 250 Å), (Å) | Total thickness, ($\pm 10\%$), (Å) | Resistivity, (20 °C), ($\pm 10\%$), ($\mu\Omega\text{-cm}$) | Conductivity, (20 °C), ($\pm 10\%$), ($\Omega\text{-cm}$) ⁻¹ | TCR, (20 to 150 °C), ($\pm 10\%$), (ppm/°C) | Gauge factor, ($\pm 5\%$), ($\delta R/R/\epsilon$) | Apparent strain sensitivity, ($\pm 10\%$), ($\mu\epsilon/^\circ\text{C}$) |
|---------|------------------------------------|------------------------------------|------------------------------------|---|--|--|--|---|--|
| KL70413 | 5000 Å ZrN | 12500 Å TiAlCr | 4400 Å ZrN+ZrON | 21900 | 184 | 5450 | -136 | --- | ----- |
| KL71024 | 2000 Å TiAlCr | 10000 Å ZrN | 3000 Å TiAlCr+PtAl | 15000 | 79 | 12640 | -7060 | 4.5 | -1570 |

4.0 Future Efforts

4.1 Diboride Films

Diborides of refractory metals are promising materials for a variety of high temperature applications, such as on leading edges of hypersonic aircraft, due to their resistance to oxidation and chemical attack. Their very high melting points earn their moniker as UHTC, and some are electrically conductive. Titanium diboride (TiB_2) is a conductive diboride that has been the subject of some research due to its attractive properties for thin film strain gauges (refs. 22 and 26). Recent studies suggest that film recession due to boria formation on the film may be an issue for temperatures above 1400 °C, particularly for porous surfaces (ref. 32).

We will continue our studies of patterned high temperature thin film strain gauges with TiB_2 targets using nitrogen as a dopant, avoiding oxygen to prevent the film recession seen with boria formation. Besides TiB_2 , zirconium diboride (ZrB_2) is another conductive UHTC attractive as a ceramic strain gauge candidate. Again, we will examine the effect of nitrogen on sputtered ZrB_2 films, determining if the TCR can be lowered to a point to make it a viable static strain gauge.

4.2 Nanostructured Films

Strain gauges of thin film conductive oxides, such as ITO, have demonstrated good drift characteristics at high temperatures, but lack the stable low TCR required for static measurements at these temperatures (refs 20 and 21). Through a NASA grant in response to a NASA Research Announcement (NRA), the University of Rhode Island recently developed a high temperature film consisting of a nanocomposite of ITO and Platinum with a reported apparent strain sensitivity of 3 $\mu\epsilon/^\circ\text{C}$ (ref. 33). These results are preliminary, and the study of the film in patterned gauges at GRC is of interest.

Another future effort planned is to incorporate ceramic nanotubes in a thin film for use as a strain gauge. Utilizing nanotubes as strain gauges have received some attention recently due to the high strain gauge factors (up to 1000) measured for stretching carbon nanotubes grown on microfabricated cantilevers (ref. 34). For a nanotube composite to be practical as a non-intrusive strain gauge on a high temperature component, the nanotubes need to be incorporated into a thin film structure oriented along the axis of strain measurement, which necessitates the development of a specialized alignment technique for the nanotubes. Of the current nanotube alignment techniques available for fabricating sensors directly on components, using an optical trap has the most potential (ref. 35). After aligning, the nanotubes will need to be coated with a compatible high temperature ceramic, such as ITO, and patterned. The issues of nanotube composition, fabrication, and composite patterning will be explored in the development of a practical fabrication process for future high temperature sensors.

5.0 Summary and Conclusions

The need for sensors to operate in harsh environments is illustrated by the need for measurements in the turbine engine hot section. The degradation and damage that develops over time in hot section components can lead to catastrophic failure. At present, the degradation processes that occur in the harsh hot section environment are poorly characterized, which hinders development of more durable components, and since it is so difficult to model turbine blade temperatures, strains, etc, actual measurements are needed. The need to

consider ceramic sensing elements is brought about by the temperature limits of metal thin film sensors in harsh environments.

The NASA GRC is pursuing the development of high temperature thin film ceramic static strain gauges for application in turbine engines, first in the fan and compressor modules, and then in the hot section. The near-term goal of this research effort is to identify candidate thin film ceramic sensor materials and outline possible thin film ceramic sensor materials and corresponding properties to test for viability. A thorough literature search was conducted for ceramics that have the potential for application as high temperature thin film strain gauges chemically and physically compatible with the NASA GRC microfabrication procedures and substrate materials.

Sputtered films of tantalum, titanium and zirconium in argon, nitrogen and oxygen gas mixes formed conductive nitrides and oxynitrides and patterned by photolithography for initial testing. The results indicate a reduction of the TCR with films sputter-deposited in argon-nitrogen environments, but with an increased instability of the films in air. Films formed by sputtering in argon-nitrogen-oxygen environments are apparently more stable in air, but suffer from slower deposition rates.

In order to have a more passive method of negating changes of resistance due to temperature, a process was developed at the NASA GRC to create a multilayer ceramic/metal thin film sensor. A first approximation model of multilayer resistance and TCR was used to set the film thicknesses in the multilayer film sensor. Multifunctional sensors were fabricated using TaN/PdCr and ZrN/TiAlCr multilayered films, and tested for low temperature resistivity, TCR and strain response. There was significant degradation of the TaN/PdCr film with time, suggesting instability of the nitride film or reaction of the nitride with chromium in the alloy. Similar effects were seen in the ZrN/TiAlCr film, but with faster degradation under low temperature heating. Apparently, an alternative method of negating the temperature sensitivity is required. Future efforts include examining the applicability of diboride films and nanostructures as high temperature ceramic thin film sensors.

References

1. Stange W., "Instrumentation Needs to Reduce Turbine Engine Related Class A Mishaps Within the USAF," *52nd International Instrumentation Symposium*, Cleveland, OH, May 7–11, 2006.
2. Lei J.F. and Will H.A., "Thin-film thermocouples and strain-gauge technologies for engine applications," *Sensors and Actuators A*, vol. 65, pp. 187–193, 1998.
3. Anson D. and Richerson D.W., "The Benefits and Challenges of the Use of Ceramics in Gas Turbines," *Progress in Ceramic Gas Turbine Development, Volume 1—Ceramic Gas Turbine Design and Test Experience*, eds. M. van Roode, M.K. Ferver, D.W. Richerson, ASME PRESS, New York, pp. 1–10, 2002.
4. Schenk B., Easley M.L. and Rickerson D.W., "Evolution of Ceramic Turbine Engine Technology at Honeywell Engines, Systems & Services," *Progress in Ceramic Gas Turbine Development, Volume 1—Ceramic Gas Turbine Design and Test Experience*, eds. M. van Roode, M.K. Ferver, D.W. Richerson, ASME PRESS, New York, pp. 77–110, 2002.
5. Levine S.R., Calomino A.M., Verrilli M.J., Thomas D.J., Halbig M.C., Opila E.J. and Ellis J.R., "Ceramic Matrix Composites (CMC) Life Prediction Development-2003," NASA/TM—2003-212493, Aug. 2003.
6. Hulse C.O., Bailey R.S., Grant H.P., Anderson W.L. and Przybyszewski J.S., "High Temperature Static Strain Gage Development," NASA CR-189044, NASA Lewis [Glenn] Research Center, p. A10, 1991.
7. Lei J.F., "High Temperature Static Strain Measurement with an Electrical Resistance Strain Gauge," AIAA-92-5039, Dec. 1992.
8. Wrbanek J.D., Fralick G.C., Martin L.C. and Blaha C.A., "A Thin Film Multifunction Sensor for Harsh Environments," NASA/TM—2001-211075. See also AIAA-2001-3315, Jul. 2001.
9. "Applications and Design of Thin Film Resistors," Vishay Electro-Films Technical Note 61083, URL: <http://www.vishay.com/docs/61083/appsdess.pdf>, [cited Nov. 2005] Dec. 2004.
10. Gerstenberg D. and Calbick C.J., "Effects of Nitrogen, Methane, and Oxygen on Structure and Electrical Properties of Thin Tantalum Films," *J. Appl. Phys.*, vol. 35 no. 2, pp. 402–407, 1964.
11. Hieber K., "Structural and Electrical Properties of Ta and Ta Nitrides Deposited by Chemical Vapour Deposition," *Thin Solid Films*, vol. 24, pp. 157–164, 1974.

12. Sun X., Kolawa E., Chen J.S., Reid J.S. and Nicolet M.A., "Properties of reactively sputter-deposited Ta-N thin films," *Thin Solid Films*, vol. 236, pp. 347–351, 1993.
13. Radhakrishnan K., Ing N.G. and Gopalakrishnan R., "Reactive sputter deposition and characterization of tantalum nitride thin films," *Mat. Sci. Eng.*, vol. B57, pp. 224–227, 1999.
14. Au C.L., Anderson W.A., Schmitz D.A., Flassayer J.C. and Collins F.M., "Stability of tantalum nitride thin film resistors," *J. Mater. Res.*, vol. 5, no. 6, p.1224, 1996.
15. Wrbanek J.D., Fralick G.C. and Gonzalez J.M., "Developing Multilayer Thin Film Strain Sensors with High Thermal Stability," NASA/TM—2006-214389. See also AIAA-2006-4580, Jul. 2006.
16. Wrbanek J.D., Fralick G.C. and Hunter G.W., "Thin Film Ceramic Strain Development for Harsh Environments," NASA/TM—2006-214466, Dec. 2006.
17. Kayser P., Godefroy J.C. and Leca L., "High-temperature thin-film strain gauges," *Sensors and Actuators A*, vols. 37–38 pp. 328–332, 1993.
18. Kazi I.H., Wilda P.M., Moor T.N. and Sayer M., "The electromechanical behavior of nichrome (80/20 wt.%) film," *Thin Solid Films*, vol. 433, pp. 337–343, 2003.
19. Gregory O.J., Bruins Slot A., Amons P.S. and Chrisman E.E., "High temperature strain gauges based on reactively sputtered AlN_x thin films," *Surface and Coatings Technology*, vol. 88, pp. 79–89, 1996.
20. Dyer S.E., Gregory O.J., Amons P.S. and Bruins Slot A., "Preparation and piezoresistive properties of reactively sputtered indium tin oxide films," *Thin Solid Films*, vol. 288, pp. 279–286, 1996.
21. Gregory O.J., You T. and Crisman E.E., "Effect of aluminum doping on the high-temperature stability and piezoresistive response of indium tin oxide strain sensors," *Thin Solid Films*, vol. 476, pp. 344–351, 2005.
22. Schultes G., Schmitt M., Goettel D. and Freitag-Weber O., "Strain sensitivity of TiB₂, TiSi₂, TaSi₂ and WSi₂ thin films as possible candidates for high temperature strain gauges," *Sensors and Actuators A*, vol. 126, pp. 287–291, 2006.
23. Wang C.M., Hsieh J.H. and Li C., "Electrical and piezoresistive properties of TaN-Cu nanocomposite thin films," *Thin Solid Films*, vols. 469–470, pp. 455–459, 2004.
24. Ayerdi I., Castaño E., Garcia-Alonso A. and Garcia F.J., "Ceramic pressure sensor based on tantalum thin film," *Sensors and Actuators A*, vols. 41–42, pp. 435–438, 1994.
25. Ayerdi I., Castaño E., Garcia-Alonso A. and Garcia F.J., "Characterization of tantalum oxynitride thin films as high temperature strain gauges," *Sensors and Actuators A*, vols. 46–47, pp. 418–421, 1995.
26. Lei J.F., Okimura H. and Brittain J.O., "Evaluation of Some Thin Film Transition Metal Compounds for High Temperature Resistance Strain Gauge Application," *Mat. Sci. Eng. A*, vol. 111, pp. 145–154, 1989.
27. Smits F. M., "Measurements of Sheet Resistivities with the Four-Point Probe," *Bell System Technical Journal*, vol. 37, pp. 711–718, 1958.
28. Blaha C.A., "Photolithographic Fine Patterning of Difficult-To-Etch Metals," NASA Tech. Briefs LEW-17079, Mar. 2002.
29. Xiong Y., Zhu S. and Wang F., "The oxidation behavior and mechanical performance of Ti60 alloy with enamel coating," *Surface & Coatings Technology*, vol. 190, pp. 195–199, 2005.
30. Dimmich R., "Electrical Conductance and Temperature Coefficient of Resistivity of Double-Layer Films," *Thin Solid Films*, vol. 158, pp. 13–24, 1988.
31. Shivaprasad S.M. and Angadi M.A., "Temperature coefficient of resistance of thin palladium films," *J. Phys., D*, vol. 13, pp. L171–2, 1980.
32. Parthasarathy T.A., Kerans R.J. and Opeka M., "A Model for the Oxidation of Refractory Diborides (Preprint)," AFRL-ML-WP-2007-464, May 2007.
33. Gregory O.J. and Chen X., "ITO-Nanocomposite Strain Gages with Low TCR," *Combinatorial Methods for High-Throughput Materials Science*, eds. by D.S. Ginley, M.J. Fasolka, A. Ludwig, and M. Lippmaa, Mater. Res. Soc. Symp. Proc., 1024E, Warrendale, PA, 1024-A05–06, 2007.
34. Cao J., Wang O. and Dai H., "Electromechanical Properties of Metallic, Quasimetallic, and Semiconducting Carbon Nanotubes under Stretching," *Physical Review Letters*, vol. 90, no. 15, Apr. 2003.
35. Plewa J., Tanner E., Mueth D.M. and Grier D.G., "Processing carbon nanotubes with holographic optical tweezers," *Optics Express*, vol. 12, no. 9, pp. 1978–1981, May 2004.

| REPORT DOCUMENTATION PAGE | | | | Form Approved OMB No. 0704-0188 | |
|--|------------------|--|-------------------------------|---|---|
| <p>The public reporting burden for this collection of information is estimated to average 1 hour per response, including the time for reviewing instructions, searching existing data sources, gathering and maintaining the data needed, and completing and reviewing the collection of information. Send comments regarding this burden estimate or any other aspect of this collection of information, including suggestions for reducing this burden, to Department of Defense, Washington Headquarters Services, Directorate for Information Operations and Reports (0704-0188), 1215 Jefferson Davis Highway, Suite 1204, Arlington, VA 22202-4302. Respondents should be aware that notwithstanding any other provision of law, no person shall be subject to any penalty for failing to comply with a collection of information if it does not display a currently valid OMB control number.</p> <p>PLEASE DO NOT RETURN YOUR FORM TO THE ABOVE ADDRESS.</p> | | | | | |
| 1. REPORT DATE (DD-MM-YYYY) 01-06-2008 | | 2. REPORT TYPE Technical Memorandum | | 3. DATES COVERED (From - To) | |
| 4. TITLE AND SUBTITLE Thin Film Ceramic Strain Sensor Development for High Temperature Environments | | | | 5a. CONTRACT NUMBER | |
| | | | | 5b. GRANT NUMBER | |
| | | | | 5c. PROGRAM ELEMENT NUMBER | |
| 6. AUTHOR(S) Wrbanek, John, D.; Fralick, Gustave, C.; Gonzalez, Jose, M.; Laster, Kimala, L. | | | | 5d. PROJECT NUMBER | |
| | | | | 5e. TASK NUMBER | |
| | | | | 5f. WORK UNIT NUMBER WBS 698259.02.07.03.02.03 | |
| 7. PERFORMING ORGANIZATION NAME(S) AND ADDRESS(ES) National Aeronautics and Space Administration John H. Glenn Research Center at Lewis Field Cleveland, Ohio 44135-3191 | | | | 8. PERFORMING ORGANIZATION REPORT NUMBER E-16519 | |
| 9. SPONSORING/MONITORING AGENCY NAME(S) AND ADDRESS(ES) National Aeronautics and Space Administration Washington, DC 20546-0001 | | | | 10. SPONSORING/MONITORS ACRONYM(S) NASA | |
| | | | | 11. SPONSORING/MONITORING REPORT NUMBER NASA/TM-2008-215256 | |
| 12. DISTRIBUTION/AVAILABILITY STATEMENT Unclassified-Unlimited Subject Category: 35 Available electronically at http://gltrs.grc.nasa.gov This publication is available from the NASA Center for AeroSpace Information, 301-621-0390 | | | | | |
| 13. SUPPLEMENTARY NOTES | | | | | |
| 14. ABSTRACT The need for sensors to operate in harsh environments is illustrated by the need for measurements in the turbine engine hot section. The degradation and damage that develops over time in hot section components can lead to catastrophic failure. At present, the degradation processes that occur in the harsh hot section environment are poorly characterized, which hinders development of more durable components, and since it is so difficult to model turbine blade temperatures, strains, etc, actual measurements are needed. The need to consider ceramic sensing elements is brought about by the temperature limits of metal thin film sensors in harsh environments. The effort at the NASA Glenn Research Center (GRC) to develop high temperature thin film ceramic static strain gauges for application in turbine engines is described, first in the fan and compressor modules, and then in the hot section. The near-term goal of this research effort was to identify candidate thin film ceramic sensor materials and provide a list of possible thin film ceramic sensor materials and corresponding properties to test for viability. A thorough literature search was conducted for ceramics that have the potential for application as high temperature thin film strain gauges chemically and physically compatible with the NASA GRCs microfabrication procedures and substrate materials. Test results are given for tantalum, titanium and zirconium-based nitride and oxynitride ceramic films. | | | | | |
| 15. SUBJECT TERMS Turbine engines; Thin films; Sensor; High temperature; Ceramics; Strain gauges | | | | | |
| 16. SECURITY CLASSIFICATION OF: | | | 17. LIMITATION OF ABSTRACT | 18. NUMBER OF PAGES | 19a. NAME OF RESPONSIBLE PERSON |
| a. REPORT U | b. ABSTRACT U | c. THIS PAGE U | | | STI Help Desk (email:help@sti.nasa.gov) |
| | | | UU | 20 | 19b. TELEPHONE NUMBER (include area code) 301-621-0390 |

